



Rheological characterization of low-calcium fly ash suspensions in alkaline silicate colloidal solutions for geopolymer concrete production

Kala Kondepudi ^a, Kolluru V.L. Subramaniam ^{b,*}

^a Department of Civil Engineering, I.I.T. Hyderabad, Hyderabad, Telangana, India

^b Dept. of Civil Engineering, I.I.T. Hyderabad, Hyderabad, Telangana, India

ARTICLE INFO

Article history:

Received 25 January 2019

Received in revised form

15 May 2019

Accepted 12 June 2019

Available online 19 June 2019

Handling editor: Vladimir Strezov

Keywords:

Alkali activated fly-ash

Geopolymer

Concrete production

Yield stress

Plastic viscosity

Thixotropy

ABSTRACT

The rheological behavior of low-calcium fly ash suspensions in activating solutions of colloidal silica and alkali hydroxide is investigated. The study is aimed at relating the rheological behavior of alkali-silicate activated low-calcium fly ash (AAF) suspensions with Portland cement paste suspensions. The yield stress and the viscosity of the AAF suspensions increase with the alkalinity of the colloidal solution, which is due to changes in the surface charges on fly ash particles with the change in the ionic medium. Increasing the alkalinity results in a less negative zeta potential of fly ash in the alkaline solution of colloidal silica and an increase in the yield stress of the AAF suspension. The thixotropic behavior in AAF suspensions is associated with structure breakdown to a finely dispersed suspension of particles produced by shearing. Energy measurements indicate a very slow change in the internal particle structure with age at room temperature. A comparison of AAF suspensions is presented with suspensions of Portland cement in water, which are proportioned for similar physical flow characteristics and yield stress. AAF suspensions have a larger solid fraction than the cement suspensions in water of comparable yield stress. The zeta potential of cement particles in water is less negative when compared to fly ash in alkaline-silicate solutions. The AAF suspensions of comparable yield stress exhibit a significantly higher viscosity than the cement suspensions in water. Cement paste and AAF suspensions exhibit a rate dependent yield response. Cement paste suspensions exhibit a threshold strain rate for minimum yield stress. In AAF suspensions there is a continuous decrease in the yield stress at lower strain rates. The thixotropic behavior in cement paste is influenced by chemical ageing which produces a rapid recovery of yield stress. In comparison, there is very little ageing at room temperature in the AAF suspensions and a very slow recovery of yield stress after shearing.

© 2019 Elsevier Ltd. All rights reserved.

1. Introduction

Concrete is one of the most used construction material, and it is conventionally made using a binder consisting of cement and water. Concrete is a particulate composite material, with aggregate inclusions in a cement paste matrix. The suspension of cement paste in water is referred to as cement paste suspension and it provides fluidity to concrete. Chemical ageing produced by the hydration reaction between cement and water produces a continuous evolution in the rheological behavior of a cement paste

* Corresponding author. Rm 310, Academic Block A, Indian Institute of Technology Hyderabad, Kandi, Sangareddy, Hyderabad, Telangana, 502285, India.

E-mail address: KVLS@iith.ac.in (K.V.L. Subramaniam).

suspension, leading ultimately to a change in the state of the material from a fluid to a solid (Subramaniam and Wang, 2010; Wang and Subramaniam, 2011). Cement paste is a non-Newtonian, shear thinning suspension which within a finite yield stress (Lootens et al., 2004; Chateau et al., 2008; Tattersall and Banfill, 1983). The rheological behavior of cement paste suspensions is well understood, and this knowledge is used to produce concrete with different flow behaviors, for diverse applications. The production of concrete with different characteristics, and for different applications such as pumping, self-levelling flow and layer deposition have been achieved by controlling the rheology of cement paste suspensions (Deng et al., 2007; Kim et al., 2017; Choi et al., 2016; Van Zijl et al., 2016; Perrot et al., 2012; Nair and Ferron, 2016; Li et al., 2002).

With the development of alternate binders, the production of concrete with a geopolymer binder instead of the conventional cement-based binder is becoming common. Geopolymers are commonly produced by activating low-calcium aluminosilicate materials such as low-calcium fly ash or metakaolin in an alkaline medium containing colloidal silica [Provis and van Deventer 2009; Bhagath Singh and Subramaniam 2017]. Low-calcium fly ash is used as the preferred source material for producing geopolymers due to its lower cost and ready availability [Palomo et al., 2014]. Understanding the rheology of the alkali-silicate activated fly ash (AAF) is becoming imminent for predicting the flow behavior of concrete with a geopolymeric binder. While the rheological behavior of cement paste system is well understood, the rheological behavior of alkali-silicate activated fly ash is still not fully established.

For producing fly ash-based geopolymers, low-calcium fly ash is activated with an alkaline activator made using a combination of alkali metal hydroxide and alkali silicate. The alkaline activator is a solution of colloidal silica, and typically, sodium-based activators consisting of sodium hydroxide (NaOH) and sodium silicate (Na_2SiO_3) are used. The activator provides the necessary alkalinity for the release of precursors from fly ash into the activated system and supplements the requirements of silica and sodium for achieving the required composition of the inorganic polymer (Duxson et al., 2007; Zhuang et al., 2016; Mucsi et al., 2018). Considerable work has been done on the optimizing the activator composition for achieving the required strength from the AAF binder. With an advancement of understanding, the optimal ratios of reactive alumina, silica and sodium and the molarity of NaOH in an AAF for achieving high strength in the geopolymer for use in structural applications have been established (Bhagath Singh and Subramaniam, 2017, 2019). Considerations of the workability requirements for processing, placement and production of concrete using AAF have however not been fully addressed.

A few studies have investigated the rheological behavior of cement-fly ash suspensions in conventional water-based pastes (Termkhajornkit and Nawa, 2004) and in alkali-silicate solutions (Laskar and Bhattacharjee, 2011; Vance et al., 2014). Influence of activating solution composition, specifically, the cation, alkalinity and silica content on the yield stress and viscosity of alkali activated fly ash have been studied. A change in the behavior of the activated fly ash suspension from Newtonian to non-Newtonian has been reported with a change in the composition of the activator suspension. With increasing silica dosage in the activator, there is an increase in the viscosity and a change to a non-Newtonian response (Vance et al., 2014). The yield stress is shown to be influenced by the cation in the solution (Vance et al., 2014). With an increase in molarity of alkaline hydroxide, there is an increase in yield stress and viscosity. AAF suspension are shown to exhibit thixotropy, which depends on the molar strength of the activating solution (Laskar and Bhattacharjee, 2011). The setting property of Alkali activated fly ash was found to be enhanced by addition of nano clay particles (Joshi et al., 2015). The rheological properties were found to be improved by adding surface reducing agents (Montes and Allouche, 2013). The superplasticizers are not as effective in the alkali-activated suspensions as in the water-based cement-paste suspensions (Criado et al., 2009; Burgos-Montes et al., 2012; Montes et al., 2012; Palacios et al., 2009).

This paper builds on the understanding of the rheological behavior of the AAF suspensions with emphasis on using sodium-based alkaline activators with low-calcium fly ash, which have been proportioned for producing stable geopolymers after hardening. The use of AAF as a replacement of cement paste suspension in producing concrete requires developing an understanding of the rheological behavior of AAF suspensions relative to cement paste suspensions. In this paper cement pastes with similar flow

characteristics obtained from physical measurements are used to establish the equivalence between ordinary Portland cement (OPC)-water suspensions and the alkali-activated fly ash suspensions. A comparison of AAF suspensions with cement suspensions provides a basis for linking the rheology of AAF suspensions with the flow behavior of concrete using the available scaling procedures developed for cement-based systems. The requirements of rheology modifiers for achieving the required flow properties from concrete made using AAF suspensions can be identified from such a study.

2. Materials and methods

2.1. Fly ash and cement

The fly ash used in this study was collected using an electrostatic precipitator in a thermal power plant. The oxide compositions of fly-ash was determined using x-ray fluorescence spectroscopy (XRF) and are listed in Table 1. The oxide contents indicate that the fly ash conforms to the requirements of Siliceous fly ash as per IS 3812 and Class F fly ash as per ASTM C618. The fly ash composition is typical of the low-calcium fly ash predominantly produced in South Asia. While the total SiO_2 and Al_2O_3 contents of the fly ash are 55.01% and 27.02%, respectively a significant portion of the available SiO_2 and Al_2O_3 are available in non-reactive, crystalline forms. The reactive SiO_2 and Al_2O_3 contents determined using the combined XRD – XRF based method were 23.41% and 16.16%, respectively (Bhagath Singh and Subramaniam, 2019). Two commercially available cements, which conformed to the requirements of Grade 53, Ordinary Portland Cement as per IS 12269 were used. The oxide compositions of the cements are also listed in Table 1. The particle size distribution of the fly ash and the cements were measured from dynamic light scattering measurements. A Microtac S3500 particle size analyser was used. Measurements were performed in isopropanol medium, and the particle size distributions are shown in Fig. 1. The cements used in the study had a larger fraction of smaller particles. The d_{50} particle size for the fly ash, Cement 1 and Cement 2 were 17 μm , 22 μm , and 40 μm , respectively.

2.2. Activating solutions

In the production of geopolymers from alkali-activation of fly ash, the fly ash is mixed with an activating solution, which is a combination of sodium hydroxide (NaOH) and sodium silicate (Na_2SiO_3). The activating solution was prepared using a commercially sourced sodium silicate. The sodium silicate contained silica in a colloidal form and the ratio of SiO_2 : Na_2O , referred to as the silica modulus (M_s) was 2.24. The mass proportions of Na_2O : SiO_2 : H_2O in the Na_2SiO_3 solution were 15.25: 34.25: 50.50. The pH of the Na_2SiO_3 solution was 12.23. The pH of the solution was found using

Table 1
Oxide compositions and physical properties of the fly ash and cements used in the study.

Oxide	Cement 1	Cement 2	Fly ash
CaO	60.46	62.88	2.63
SiO_2	20.24	19.66	55.01
Al_2O_3	5.78	4.63	27.015
Fe_2O_3	4.20	4.36	7.47
MgO	1.06	1.04	1.34
K_2O	1.12	1.01	2.565
SO_3	2.36	1.44	0.615
TiO_2	0.31	0.46	1.97
P_2O_5	0.18	0.20	0.52
MnO	0.00	0.11	0.03

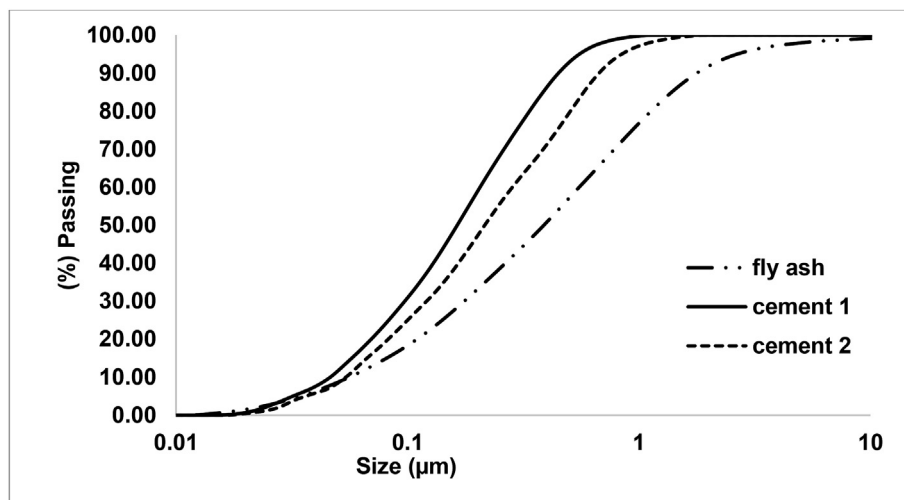


Fig. 1. Particle size distributions of fly ash and cement powders.

a pH meter of Metrohm make. The pH meter was calibrated with known solutions and then the electrode was immersed into the sodium silicate solution for a sufficiently long time until a stable pH value was obtained. The alkaline activating solutions were prepared by mixing sodium silicate solution with NaOH solution made using 98% reagent grade NaOH pellets.

The alkaline activating solution was proportioned based on the requirement of precursors to produce stable geopolymers. The compositions of solutions were decided based on optimum values required for achieving high strength from alkali-activation of the fly ash used in the study (Bhagath Singh and Subramaniam, 2017, 2018). The requirements of Na_2SiO_3 and NaOH were decided based on achieving reactive oxide ratios in the activated system consisting of fly ash and sodium-based alkaline solution. The reactive silica in the activated system consists of the reactive silica supplied by the dissolution of fly ash and the colloidal silica from Na_2SiO_3 in the activating solution. In the activated system, fly ash is the source of reactive alumina. The activating solution was prepared to achieve a reactive oxide ratio of $\text{SiO}_2/\text{Al}_2\text{O}_3$ close to 2.0 in the activated system (Bhagath Singh and Subramaniam, 2017). The amount of NaOH was determined to achieve a ratio of $\text{Na}_2\text{O}/\text{reactive Al}_2\text{O}_3$ greater than a threshold value of 0.2 (Bhagath Singh and Subramaniam, 2017). The water was adjusted to maintain a molarity of NaOH greater than 3.0M based on the requirement for achieving complete dissolution of the glassy phase in fly ash (Bhagath Singh and Subramaniam, 2017; Bhagath Singh et al., 2018). For the fly ash used in the study, the activating solutions, which were proportioned for the optimum oxide ratios to achieve stable geopolymers from the fly ash are given in Table 2. Two different activating solutions with different molarities of NaOH equal to 3.0M and 5.6M were prepared. The definition of molarity used here refers to the number of moles of NaOH in 1000 g of water. The physical quantity

of water in the activating solutions as a proportion of the remaining constituents, the NaOH and the Na_2O and SiO_2 from the Na_2SiO_3 solution was kept constant as shown in Table 2. The water in the sodium-based alkaline activation solution consists of the water contributed by the Na_2SiO_3 solution and the water added to achieve the required molarity of NaOH. The two activating solutions had identical silica and water contents and differed in molarity of NaOH. The two solutions allow for evaluating the influence of NaOH on the rheological properties of AAF suspensions.

2.3. Alkali-activated fly ash suspensions

Two AAF suspensions were prepared by mixing fly ash with the alkaline activating solutions such that the mass proportions of water to solids in the suspensions was equal to 0.21. The AAF-3.0 and AAF-5.6 suspensions were prepared using the 3.0M NaOH and the 5.6M NaOH activating solutions, respectively. The different ratios of constituents in the AAF suspensions are given in Table 3. The solids in the AAF suspension consisted of fly ash, the NaOH and the Na_2O and SiO_2 contents in the sodium silicate solution. In the AAF suspension, the fly ash is identified as the binder solid. The fly ash was mixed with the 3.0M and the 5.6M NaOH activating solutions in the mass proportions of binder solid: activating solution equal to 1:0.40 and 1:0.43. The volumetric proportion of binder solid to the activating solution, which represents the solid loading of the AAF-3.0 and the AAF-5.6 suspensions were 1:0.67 and 1:0.70, respectively. The two AAF suspensions had very different consistencies and allowed for evaluating the influence of solution composition while keeping all other variables constant. The solid volume fractions of the two suspensions are also comparable. The solid volume fractions of the AAF-3.0 and the AAF-5.6 suspensions were 0.59 and 0.6, respectively. The reactive oxide ratios in the AAF

Table 2

Compositions of activating solutions for alkali-activated fly ash suspensions (mass basis) for 100 g of fly-ash.

Activating Solution	Additional Water* (g)	NaOH (g)	Na_2SiO_3 solution** (g)	Molarity of NaOH	Specific gravity of activating solution ***
3.0M NaOH Activating Solution	11.5	3.04	26	3.0 M	1.37
5.6M NaOH Activating Solution	11.3	5.8	26	5.6 M	1.40

* The additional water for achieving the molarity of NaOH.

** Solution with M_s 2.24 (mass proportion of $\text{Na}_2\text{O}:\text{SiO}_2:\text{H}_2\text{O} = 15.25:34.25:50.5$).

***Activating solution: Sodium silicate + amount of water needed to obtain the molarity + sodium hydroxide.

Table 3
Physical properties and compositions of the AAF and cement paste suspensions.

Suspension	Designation	Mixing solution	Binder solid	solution/binder solid (Volume ratio)	Solution/Binder solid (mass ratio)	Water/solids* (mass ratio)
AAF	AAF-3.0	3M NaOH Activating Solution	Fly ash	0.67:1.0	0.40	0.21
	AAF-5.6	5.6M NaOH Activating solution	Fly ash	0.7:1.0	0.43	0.21
Cement paste	C2-0.3	Water	Cement 2	0.94:1.0	0.3	0.30
	C1-0.4	Water	Cement 1	1.26:1.0	0.4	0.40

* Solids in AAF are Fly-ash + sodium hydroxide + sodium oxide and silica from sodium silicate.

*Solids in cement paste suspension refer to cement.

suspensions, considering the reactive species contributed by fly ash and the activating solution are given in Table 4. In the AAF suspensions, the reactive oxide ratios of $\text{SiO}_2/\text{Al}_2\text{O}_3$ were close to 2.0 and the ratios of $\text{Na}_2\text{O}/\text{reactive Al}_2\text{O}_3$ were greater than the threshold value of 0.2.

2.4. Cement paste suspensions

Suspensions of ordinary Portland cement in water (referred to as cement paste suspensions) were proportioned to provide a basis for comparison between the AAF and the cement systems. Cement paste suspensions were prepared by mixing cement powder with water to achieve similar physical flow characteristics as the AAF suspensions. The mini slump cone was used to provide a basis for comparison between the AAF and the cement paste suspensions. The mini-slump cone is a truncated cone with the proportions of height: base diameter: top diameter equal to 1.5: 2: 1. In the mini slump test, the mould is filled with paste, and the cone is lifted without inertial effect. The flow comes to a rest as the shear stresses produced by the gravity induced flow are overcome by the internal resistance generated within the material, to reach a stable structure (Kantro, 1980). The dimensions of the final shape of the suspension at rest, the diameter of spread or the slump, which is the decrease in the height of the suspension at rest compared to the initial height of the cone, are measured. The spread diameter of cement paste suspensions has been shown to correlate well with its yield stress obtained from rheological measurements (Roussel and Coussot, 2005; Pierre et al., 2013; Tan et al., 2017). The mass ratio of water to cement (w/c ratio) of the cement paste suspension was varied to achieve similar behavior as that of the AAF suspensions in the mini-slump test. A mini-slump cone mould of dimensions (top diameter) x (bottom diameter) x (height) of $5 \times 10 \times 7.5$ cm was used in this study, and the spread diameter or slump was measured. The spread diameter was measured orthogonally in two directions, and the average value was taken. The slump measurement indicates the direct vertical subsidence of the suspension at rest.

2.5. Mixing and testing procedures

The rheological measurements were performed on the suspensions using a AR-G2 strain-controlled rheometer with a concentric vane measurement system. The diameter of the cup was 30 mm, and a four bladed vane of 28 mm diameter was used. The cup and vane geometry was used for the measurement purpose since it has been shown to be effective in water-based suspensions,

such as cement paste where measurements are influenced by slip. Slip results from the formation of a water rich layer at the surfaces and is prominent in the parallel plate and the concentric cylinder geometries (Saak et al., 2001; Olivas et al., 2016). All rheological measurements were performed at a constant temperature of 27°C.

The AAF suspensions were prepared by mixing the activating solutions with fly ash using a paddle mixer. The AAF suspension was mixed at 300 rpm for two and half minutes and the sample was placed in the concentric cylinder with in 60s after the mixing. A pre-shear of 20s^{-1} was applied for 300s followed by a 120s equilibration time before initiating measurements. Different measurement protocols, which have been used for rheological characterization of cement suspensions were used to investigate the yield the shear thinning, and the thixotropic behaviors. The test procedures used to evaluate the rheological behavior of the AAF and cement suspensions are shown in Fig. 2 and are as follows: (a) Constant shear rate test (Constant angular velocity); (b) Hysteresis test; (c) Equilibrium test; (d) Equilibrium followed by a hysteresis test. In the constant shear rate test, the shear stress was measured with a constant applied angular velocity. Constant angular velocity tests were performed at different constant angular velocities ranging from 0.001 rad/s to 1 rad/s. The constant shear rate tests were used to study the yield behavior of cement suspensions (Saak et al., 2004). The yield stress was identified with the onset of flow as the angular strain was increased. In a hysteresis test, the shear rate was ramped up from zero to a prescribed value and then ramped down to zero again. The ramp rate used in this study was 0.33 s^{-2} with a total time of 240s. The deviation from the Newtonian behavior and the sensitivity of shear rate is established from these tests (Frigaard et al., 2017). The Bingham model was fitted to the ramp down curve between shear rates ranging from 10 s^{-1} to 30 s^{-1} as

$$\tau = \tau_0 + \mu \left(\frac{du}{dy} \right) \quad (1)$$

where du/dy is the shear rate, τ_0 is the shear stress required to initiate the flow, and μ is the constant of proportionality identified with plastic viscosity.

In the equilibrium test, the shear rate was ramped up from 0 to 40 s^{-1} in 120 s followed by application of constant shear rate. The shear rate was held constant at 40 s^{-1} until equilibrium was achieved. The duration of time, $t_{\text{equilibrium}}$, was determined when the shear stress from the structural breakdown attained a constant value at the applied strain rate. After attaining equilibrium, the

Table 4
The oxide compositions (mass ratios) based on the reactive components in the AAF suspensions.

AAF suspension	(reactive SiO_2 from fly ash + SiO_2 from Na_2SiO_3)/(reactive Al_2O_3 from fly ash)	Na_2O (Reactive Al_2O_3)
AAF-3.0	2	0.2
AAF-5.6	1.8	0.25

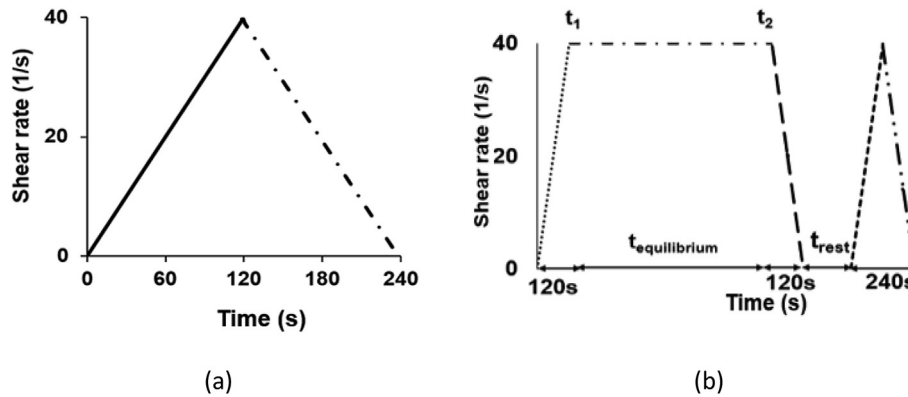


Fig. 2. Test protocols followed in the test program: (a) Hysteresis loop test; (b) Equilibrium test followed by a hysteresis test.

shear rate was ramped down to zero at a ramp rate of 0.33 s^{-2} . The hysteresis loop test was conducted on the sample after different rest periods ranging from 0 to 30 min. A new sample was used for each test for a given rest period. This test allows for evaluating the thixotropic response of the suspension, which is sheared to an equilibrium state at a constant shear rate. The material state after the structure breaks down represents a reference state for evaluating the structure buildup in the suspension.

2.6. Zeta potential measurements

The zeta potential of the fly ash particles was measured in different solution media to assess the stability of the suspension. Zeta potential measurements of the fly ash were performed using solutions of NaOH of different molarities and solutions of Na_2SiO_3 with NaOH. Deionized water was used for establishing the reference. NaOH solutions of 0.1M and 0.5M were used. Considering the limitations imposed by the very viscous nature of the Na_2SiO_3 solution, the Na_2SiO_3 solution was diluted in water. Water was added to 26 g of the Na_2SiO_3 solution to a total mass of 100 g. For solutions of Na_2SiO_3 and NaOH, the Na_2SiO_3 solution was mixed with NaOH and diluted with water to achieve two different molarities of NaOH in the solution equal to 0.1M and the 0.5M. The pH of the Na_2SiO_3 solution after adding NaOH increased from 12.23 to 12.91. A Malvern Zeta sizer nano ZS90 model instrument was used to determine the Zeta potential of the fly ash in the different solutions. To measure zeta potential, a re-useable folded capillary zeta cell was used. The sample was injected into the plugs of the capillary zeta cell. In a typical measurement, the movement of the

particles under the influence of an applied potential field is used to determine the zeta potential.

3. Results and discussions

A comparison of the spread diameter and the slump of the AAF and cement paste suspensions are shown in Figs. 3 and 4. The AAF suspension with the 3.0M activating solution exhibited a complete collapse and a spread with a diameter equal to 14.65 cm. A cement paste suspension with a spread diameter equal to 14.15 cm was achieved using Cement 1 mixed with water in the mass proportion of water to binder solid (w/c) equal to 0.4. The volumetric ratio of the solution to binder solid of the cement suspension was 0.94:1 when compared to 0.67:1 in the AAF-3.0 solution. The AAF suspension with the 5.6M activating solution exhibited a slump with a subsidence equal to 5.5 cm. A cement paste suspension with a slump equal to 5.5 cm was achieved using Cement 2 mixed with water in a water-to-binder solid (w/c) mass proportion of 0.3. The volumetric ratio of solution-to-binder in the cement suspension was 1.26:1.0 when compared to 0.7:1.0 in the AAF-5.6 solution. The volumetric and mass proportions of the binder for the cement paste and AAF suspensions proportioned for similar mini-slump behavior are listed in Table 3. Both cement paste and fly ash suspensions have a high solid fraction with particles in size range including the colloidal and the non-colloidal. Comparing the AAF and cement paste suspensions, AAF suspensions have a significantly higher solid volume fractions than the corresponding cement paste suspensions. Cement paste suspensions with w/c ratios equal to 0.3 and 0.4 have been conventionally used for evaluating cement paste



Fig. 3. Comparison of spread diameters from the mini slump test: (a) C1-0.4 suspension with a 14.15 cm flow diameter; (b) AAF-3.0 suspension with a 14.62 cm flow diameter.

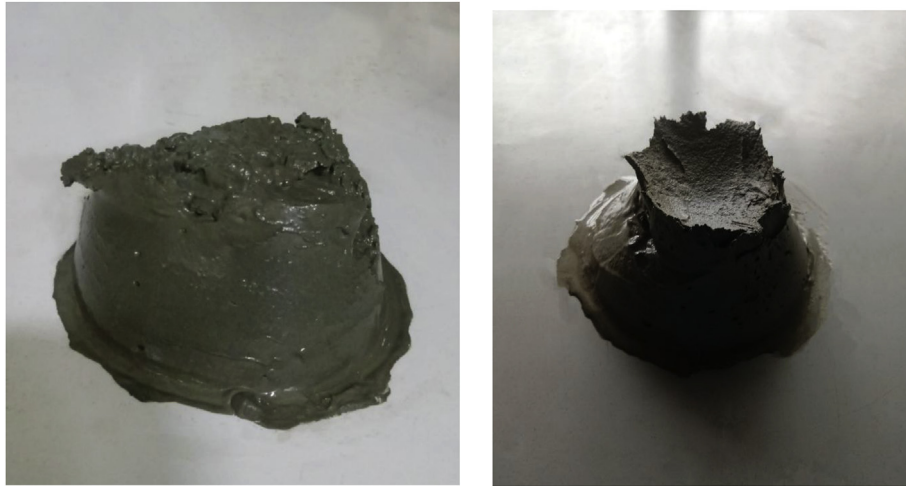


Fig. 4. Comparison of slump from the mini slump test b: (a) C2-0.3 suspension with a 5.5 cm slump; (b) AAF-5.6 suspension with a 5.5 cm slump.

systems because of the range of fluidity available with the change in the solid loading (Ray et al., 2015). The w/c ratios are conventionally varied within the range between 0.3 and 0.4 in producing concrete with the suitable use of rheology modifiers.

The mean zeta potential and the corresponding standard deviation values obtained from fly ash dispersed in the different media are given in Table 5. The standard deviations are within ten percent of the mean values. Fly ash has a large negative zeta potential in water indicating that the dispersion of fly ash in water is stable with a low instability to the dispersed state due to agglomeration or coagulation of particles. The magnitude of potential, which indicates the degree of electrostatic repulsion between the adjacent similarly charged particles decreases with an increase in the molarity of NaOH. A less negative zeta-potential is indicative of an increase in the attractive forces between the particles, which favors flocculation in the system. The addition of Na_2SiO_3 to NaOH results in more negative zeta potential than the corresponding NaOH solution, which increases the stability of the dispersion. The increase in the zeta potential with the addition of Na_2SiO_3 is likely due to the increase in the silica content in the suspension.

3.1. Rheological characterization of alkaline activating solution

The flow curves of the 3.0M and the 5.6M NaOH activating solutions up to an applied strain rate of 100s^{-1} indicated a Newtonian behavior. The viscosity of the 3.0M and 5.6M NaOH activating solutions were equal to 0.042 Pa and 0.075 Pa, respectively. Sodium silicate is made from a salt of a weak acid and strong base and hence has a pH in the range between 10 and 13. The sodium silicate solution exhibits the lowest viscosity for an M_s , the $\text{SiO}_2:\text{Na}_2\text{O}$ ratio close to 1.8 (Yang et al., 2008). The viscosity increases on making the solution more siliceous or more alkaline. In the solution, there are colloidal particles in different size ranges with different degrees

of condensation. The size of the colloidal particles is determined by the condensation of Si to form structures with Si–O–Si linkages. Increasing the siliceous content results in larger colloidal particles of higher molecular mass with higher level of Si–O–Si linkages. Increasing the alkalinity with the addition of Na favors the formation of smaller colloidal particles in the size range less than 10 nm, which have large surface area (Yang et al., 2008). The M_s of sodium silicate solution used in this study had an M_s equal to 2.24. Addition of NaOH at 3.0M and 5.6M increases the Na content and reduces the M_s lower than the threshold value of 1.8. For the range of M_s less than 1.8, an increase in molarity of NaOH produces an increase in the viscosity of the solution. The increase in viscosity is due to the increasing surface area of the finer sized colloidal particles in silica suspensions with an increase in the sodium content.

3.2. Constant shear rate test

The stress as a function of time measured at different applied strain rates from the constant shear rate tests on different suspensions are shown in Fig. 5 (a) and (b). The stress attains a peak following initial rise, which is identified as the yield stress. The yield stress defines the onset of flow, which occurs when the material is sheared past a critical strain (Roussel et al., 2012). Both AAF and cement paste suspensions exhibit rate sensitivity in the initial response and the yield stress. A stiffer response is obtained at a higher strain rate. At high shear rates, the rate of strain application is faster. At short time scales, the system cannot adjust itself fast enough, producing a stiffer response. There is a fundamental difference in the yield stress measured at different strain rates exhibited by the cement paste and the AAF suspensions. While cement paste suspensions exhibit a decrease followed by an increase in the yield stress on decreasing the strain rate, the AAF suspensions exhibit a continuous decrease in the yield stress with decreasing shear rate.

The rate dependence of yield stress in the AAF and cement paste suspensions is shown in Fig. 6 (a) and (b). Starting from angular velocity on the order of 1 rad/s, both AAF and cement paste suspensions initially exhibit a decreasing yield stress with decreasing angular velocity. With decreasing strain rate, the cement paste suspensions exhibit a minimum in the yield stress followed by an increasing yield stress at lower shear rates. The rate dependence of yield stress in cement has been attributed to structural buildup and structure assembly driven by the interaction potentials and

Table 5
Zeta potential of fly ash in different dispersants.

Dispersant	Zeta-potential, mV Mean (std. dev.)
Water	–29.2 (0.5)
0.1M NaOH	–19.16(0.4)
0.5M NaOH	–17.0(0.62)
Sodium silicate (dilute)+0.1M NaOH	–20.5(2.35)
Sodium silicate (dilute)+0.5M NaOH	–19.9(2.18)

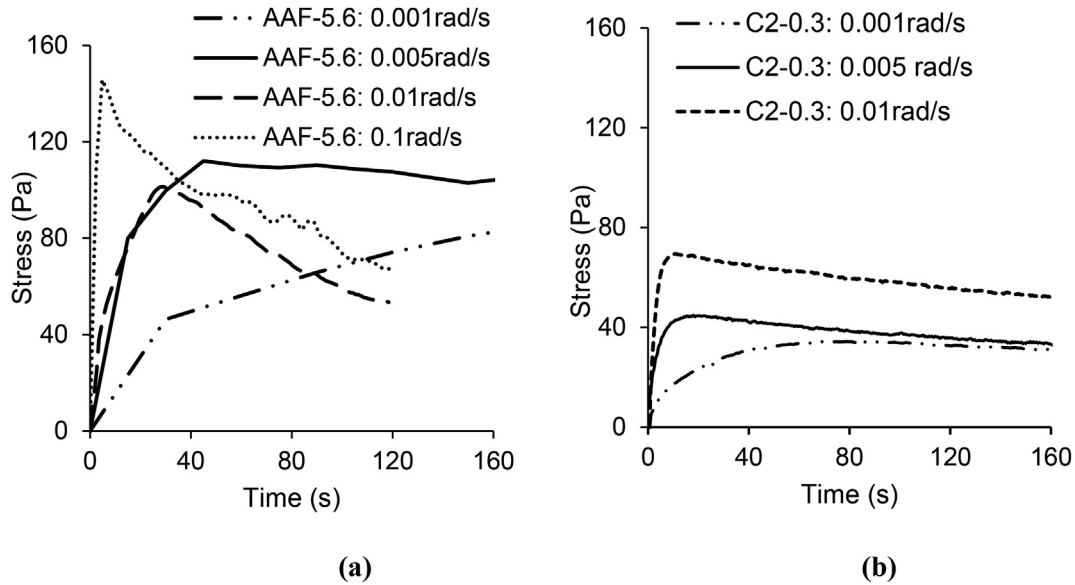


Fig. 5. Shear stress as a function of time in constant angular velocity tests: (a) AAF-5.6 suspensions; (b) C2-0.3 suspensions.

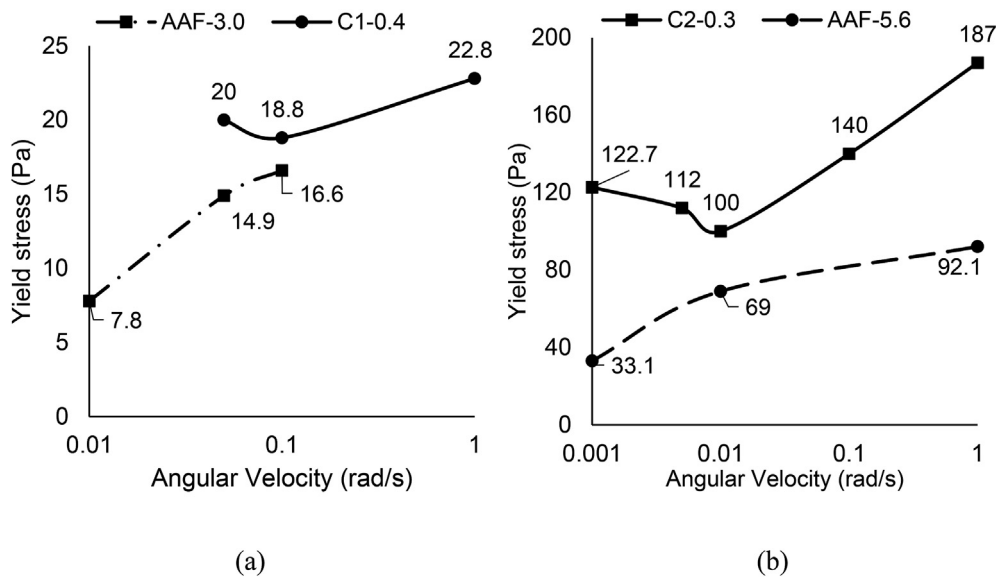


Fig. 6. Variation of yield stress with angular velocity: (a) for C1-0.4 and AAF-3.0 suspensions; (b) for C2-0.3 and AAF-5.6 suspensions.

chemical bonding between the colloidal particles. This has been linked to thixotropy of the material (Yuan et al., 2017). At a small angular velocity, the duration of test needs to be long enough in order to break the structural bonds between the particles. This makes the cement paste suspensions withstand higher stresses before yielding due to the reorientation of particles (Saak, et al., 2000). The inter-particle potential in cement paste suspensions with w/c ratios in the range 0.3–0.4 are low, in the range of -7 mV– 12 mV (Lowke and Gehlen, 2017). The low zeta potential in the suspensions with high solid fractions favors agglomeration. In cement paste suspensions, the structural buildup and reorientation occurs on a time scale which is comparable to the time required for the material reach the critical strain at lower strain rates (Saak, et al., 2000; Kim et al., 2016). At higher rotational speeds, less time duration is sufficient to attain the critical strain. The rapid increase in stress is linked to the dynamic response of the internal structure (Saak, et al., 2000). In AAF suspensions, the continued decrease in

the yield stress at flow initiation with decreasing shear rate suggests the continuous reorientation of the internal structure and a viscoplastic deformation produced by the highly viscous activating fluid between the fly ash particles. Fly ash contains spherical particles, which can arrive at a 3D structure by rotation before a complete breakdown of the internal structure. At the very low strain rates and the large time scales involved, the system can continuously adjust itself to produce a creep type behavior (Barnes, 1997).

The yield type behavior in the suspensions with high particle volumes, is associated with the existence of an internal structure of particles, which is capable of resisting finite stress. The three-dimensional network of particles with a long-range order has been verified using ultrasonic measurements on cement paste suspensions with different solid concentrations (Subramaniam and Wang, 2010; Wang and Subramaniam, 2011). The at-rest structure of solid particles is broken down with shearing. With increasing

strain, flow is induced in the suspension beyond a critical strain with the rearrangement and large relative movement of particles (Kim et al., 2016). The yield behavior of cement suspensions is attributed to colloidal particle interaction and the particle bridging at the points of contacts on the solid network provided by reaction products (Roussel and Coussot, 2005). In cement suspensions, there is an increase in the yield stress with an increase in the solid fraction in the suspension. The decrease in the inter-particle distance with an increase in solid loading and the low inter-particle zeta potential in cement paste suspensions with w/c ratio in the range 0.3–0.4 favor an agglomerated structure (Lowke and Gehlen, 2017). An increase in the solid volume fraction leads to a more percolated system of particles with a longer range order, which is capable of resisting higher shear.

The yield type behavior exhibited by the AAF suspensions is attributed to the inter-particle forces associated with the interaction potential, the viscosity of the activating solution and the existence of a particle network with a long-range order (Vance et al., 2014). In the two AAF suspensions, which had similar solid loading, the yield stress increases with the molarity of NaOH. The stability of the suspension in the dielectric medium is determined by the electrostatic repulsive and the attractive van der Waals potentials. The electrostatic potential, which is indicated by the zeta potential is dependent on ionic concentration (Yotsumoto and Yoon, 1993). The van der Waals potential does not depend on the ionic strength. The zeta potential controls the inter-particle interaction with changing molarity. The decrease in the zeta potential suggests a higher potential for agglomeration with an increase in molarity of NaOH. Higher yield stress in solutions with a higher molarity of NaOH is linked to the higher tendency of the fly ash to agglomerate.

The yield stress in the cement paste and the AAF suspensions, which were conditioned for similar slump have comparable yield stress values at the threshold strain rate of cement paste suspensions. Comparing the cement and the AAF suspensions, comparable yield is achieved at a higher solid loading in AAF suspensions. The local spatial rearrangement of the spherical particles present in fly ash before a complete breakdown of the internal structure is less influenced by shearing, resulting in a lower yield stress.

3.3. Hysteresis test

The stress as a function of shear rate from the hysteresis tests on

different suspensions are shown in Fig. 7 (a) and (b). The yield type behavior is evident at the low strain rates. The flow following the initial yield exhibits a shear-thinning-type behavior. The plastic viscosity determined from the Bingham model fit to the downward loop of the hysteresic response are listed in Table 6. The viscosity of the AAF-5.6M suspension is significantly higher than the AAF-3.0M suspension. Since the solid volume fractions are not significantly different between the two AAF suspensions, the differences are attributed to the differences in the viscosities of the activating solutions of different molarities. Comparing suspensions of comparable yield stress, the viscosity of the AAF suspension is significantly higher than the viscosity of the cement paste suspension. In cement paste suspensions there is an increase in viscosity on increasing the solid loading.

Particulate suspensions exhibit a shear thinning behavior due the interaction between the fluid medium and the shearing and realignment of particles, particle-particle interaction stress and a hydrodynamic component of the shear flow of the fluid (Bender and Wagner, 1995). The Brownian effects are usually negligible over the range of shear rates of up to 100s^{-1} (Bender and Wagner, 1995; Foss and Brady, 2000; Singh and Nott, 2003). On shearing, the internal structure in cement paste suspension associated with the long-range order produces flocs associated with short-range forces of interaction between particles (Kim et al., 2016). As a flocculated suspension of particles, cement paste exhibits a shear thinning behavior, which is associated with behavior of flocs in a Newtonian fluid medium resulting from a decrease in the size of these structures at increasing shear rate (Dai et al., 2013; Kim et al., 2016). In the AAF suspension, the activating solutions exhibit a Newtonian behavior over the range of shear rates $0\text{--}100\text{s}^{-1}$. The larger viscosity of the activating solution results in higher shearing stresses on the particle flocs in AAF suspensions. Additional contribution to the shear thinning response comes from the hydrodynamic flow

Table 6
Viscosity and yield stress of the AAF and cement paste suspensions.

Material	Viscosity (Pa.s)
C1-0.4	0.91
C2-0.3	1
AAF-3.0M	15.11
AAF-5.6M	24.3

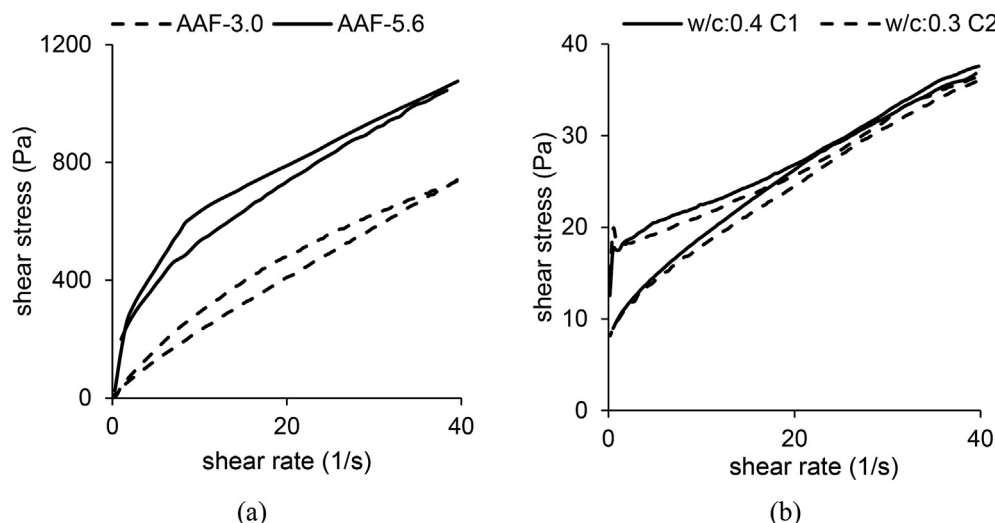


Fig. 7. Shear thinning behavior of: (a) AAF-5.6 and AAF-3.0 suspensions; (b) C2-0.3 and C1-0.4 suspensions.

induced between the fly ash particles (Zarraga et al., 2000; Lin et al., 2015). In a suspension with a very high solid particle loading, subjected to an applied strain rate in the range of $10\text{--}100\text{s}^{-1}$, the local shear rate of the activating fluid between the particles is significantly higher, where the fluid exhibits a shear thinning behavior. In high particulate suspensions of silicone, the local shear rate experienced by the fluid between the particles was significantly larger than the average shear rate of the whole suspension, where the suspension exhibits shear thinning behavior (Vázquez-Quesada et al., 2016).

3.4. Equilibrium test

The shear stress as a function of applied shear rate obtained from equilibrium tests on cement paste and AAF suspensions are plotted in Fig. 8. The flow curves at a constant shear rate of 40s^{-1} are shown in the insets. The constant shear rate tests were performed till a constant value of shear stress was obtained. The shearing time required to achieve a constant viscosity varied with suspension. From five replicates, the shearing time required to

achieve constant viscosity were 515s, 606s, 480, and 450s for the AAF-3.0, AAF-5.6, C2-0.4 and C1-0.3 suspensions, respectively. The reduction in the viscosity under shearing at a constant shear rate is indicative of breakdown of the structure and attainment of an equilibrium state at the applied shear rate. In the equilibrium state the flocculated structure reaches a constant state where the structural breakdown produced by the applied shearing is balanced by the forces which lead to flocculation, resulting in the lowest energy state. A hysteresis loop is formed upon ramping the shear rate down to zero. The state of the material after completing the hysteric loop represents a reference state for evaluating the rate of structure buildup. The ramp down curve represents an equilibrium line connecting the reference state and the equilibrium state.

The structure buildup was evaluated by testing the suspension after different rest periods, t_{rest} , from the equilibrium state. The increase in shear stress with increasing shear rate after different rest periods, is shown in Fig. 9 (a) and (b) for the AAF-5.6 and the C2-0.3 suspensions, respectively. The behavior at the low shear rates is shown in the inset for clarity. The low shear rate behavior indicates a recovery of yield stress with increasing rest period. In

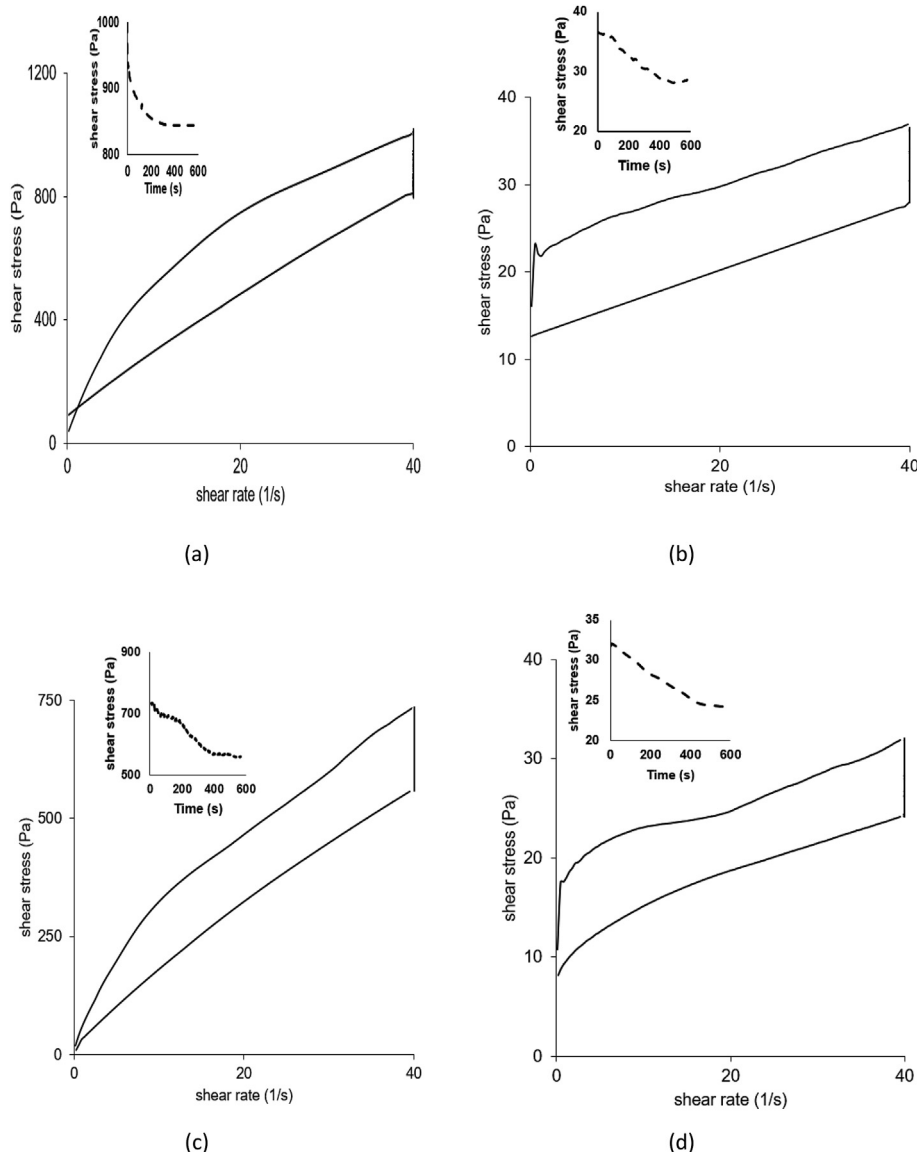


Fig. 8. Thixotropy equilibrium test: (a) AAF-5.6; (b) C2-0.3; (c) AAF -3.0; (d) C1-0.4. The inserts in the figure represent the equilibrium curves of respective flow curves.

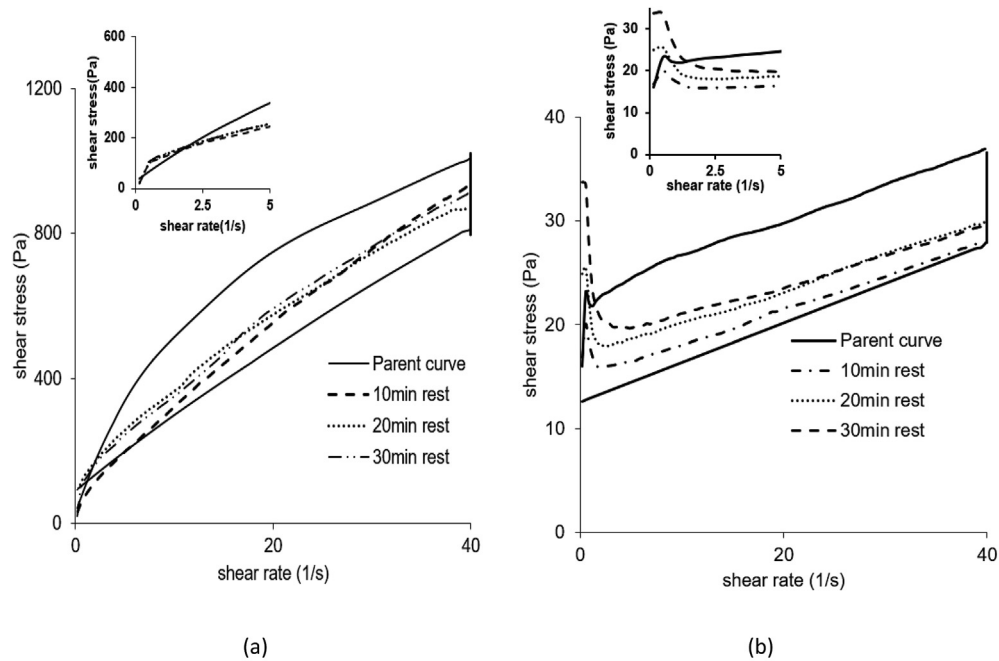


Fig. 9. Equilibrium hysteresis loop and the shear ramp after different rest periods: (a) AAF-5.6; (b) thixotropy test of C2-0.3.

the cement paste suspensions, the yield stress is recovered rapidly within the first 10 min. The yield stress continues to increase beyond the initial yield stress after 10 min. In the AAF suspension, the recovery of yield is slow and even after 30 min the initial yield stress is not recovered.

To evaluate the rebuilding of the flocculated structure with time, the area between the up ramp after a defined rest period and the equilibrium line was calculated at shear rates associated with flow after the initial yield behavior. The area between the up ramp and the equilibrium line was calculated between shear rates equal to 10 and 30s^{-1} and is referred to as the specific rebuilding energy (SRE) (Ferron et al., 2007). The SRE gives a measure of rebuilding of the flocculated structure and the evolution of viscosity in the system from a reference state defined by the equilibrium line. To provide a reference, the area under the equilibrium line was computed between shear rates of 10 and 30s^{-1} and is referred to as the equilibrium area. The SRE normalized with the equilibrium area is plotted in Fig. 10 for the AAF and cement suspensions. The non-

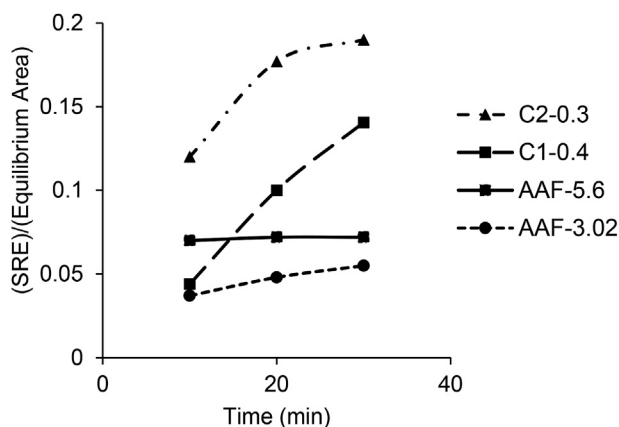


Fig. 10. Normalized structural rebuilding energy as a function of rest period after equilibrium.

dimensional measure of SRE indicates a significantly more rapid buildup in cement paste suspensions when compared with the AAF suspensions. The buildup indicated in the figure is for the flow regime past the yield stress. The available data indicates that past the yield stress, there is an insignificant change in the particle structure in the AAF suspensions with age. The change in the SRE recorded from AAF suspension is an order of magnitude slower than the change recorded from cement paste suspensions.

The thixotropic measurements in cement paste contain influences of both reversible flocculation and chemical ageing effect (Feys et al., 2007, Ferron 2008). The recovery of yield stress is due to the buildup of a structure with a long range order of percolated grains, which is capable of transmitting shear stress. In cement paste suspensions, structural linkages are formed preferentially at the points of contact particles (Roussel et al., 2012). This ageing effect is significant in cement paste suspensions and it contributes to the rapid increase in yield stress (Roussel et al., 2012). The increase in the chemical linkages is associated with chemical ageing and produces an irreversible loss of workability, leading eventually to setting of the material. In the ageing system, the flocculated particles created in the suspension on shearing past the yield stress are associated with short-range forces due to van der Waals forces and also due to the chemical linkages formed between particles, which are termed as reversible and irreversible coagulation (Wallevik, 2005). In cement suspensions, the thixotropic behavior is associated with the decrease in the floc size from both reversible and irreversible effects (Raissa et al. 2007).

In the AAF suspensions, a finely dispersed suspension of particles is created by shearing. After shearing, the reassembly of an internal structure leading to a percolated network of particles with a long range order promoted by the electrostatic and van der Waals forces is slow to develop. In AAF suspensions, the activation of fly ash, which leads to a release of reactive species and the formation of reaction products is achieved at temperature higher than $30\text{ }^{\circ}\text{C}$. At $27\text{ }^{\circ}\text{C}$, there is little or no reaction or chemical activity and the dissolution of chemical species does not occur till significantly later (Bhagath Singh and Subramaniam, 2019). Therefore, the buildup of

internal structure is associated only with the stability of the dispersed particles in the solution.

4. Summary and findings

The findings of this study allow for extending the previous accumulated knowledge from the use of cement paste suspensions in producing concrete to AAF suspensions. In concrete made with cement paste suspensions, the rheology is controlled for different applications such as pumping with the use of admixtures (Kong et al. 2013). Additionally, methods for assessing the flow of concrete for specific applications have also been developed (Perrot et al., 2012). In cement paste suspensions, the rapid increase in the structural linkages which contributes to a rapid increase in yield stress is used for an advantage in layer deposition based printing procedures with the use of chemical accelerators to produce a set on demand-type material. Extension of the existing knowledge for use with AAF suspensions requires the considerations of the main findings obtained in this paper, which are given below.

AAF suspensions exhibit a non-Newtonian behavior with a definite yield stress and shear thinning for increasing shear rates. The rheology of the AAF suspension is strongly controlled by the activating solution. The activating solution exhibits increasing viscosity with increasing sodium and silica contents. Increasing the molarity of NaOH increases the zeta potential of fly ash in the activating solution favouring aggregation. This leads to increases in the yield stress and the viscosity of the AAF suspension. In AAF suspensions, the rheology for a given solid fraction can be controlled by changing the molarity of NaOH in the solution. An increase in yield stress is produced for the same solid volume fraction, with an increase in the molarity of the activating solution.

Cement paste suspension and AAF suspensions proportioned for identical physical gravity induced flow behavior gives similar yield stress. Cement paste and AAF suspensions with similar yield stress have different viscosities. For comparable yield stress, the AAF suspension has a significantly higher viscosity. Yield stress comparable to cement paste suspensions is obtained at a higher solid volume fraction in AAF suspensions. In cement paste suspensions, an increase in yield stress is achieved with an increase in the solid volume fraction.

The yield stress of AAF suspensions exhibits a continuous decrease with the shear rate. In cement paste suspensions, with an increase in the shear rate, the inertial effects increase the yield stress, whereas at lower shear rate the structural build up results in a higher yield stress. The decrease in the yield stress of the AAF suspensions at lower strain rates is due to the viscoplastic deformation produced by the highly viscous activating solution between the fly ash particles.

Thixotropic behaviors in both AAF and cement paste suspensions produce a decreasing viscosity at a constant shear rate. The yield stress recovery is slow in AAF suspensions, while in cement paste suspensions, there is a significant increase in yield stress due to ageing effects.

Acknowledgements

The authors would like to acknowledge support from the Department of Science and Technology, Initiative to Promote Energy Efficient Habitant (I-PHEE) Grant No. TMD/CERI/BEE/2016/031.

Appendix A. Supplementary data

Supplementary data to this article can be found online at <https://doi.org/10.1016/j.jclepro.2019.06.124>.

Compliance with ethical standards

The authors declare that they have no conflict of interest.

References

- Barnes, H.A., 1997. Thixotropy—a review. *J. Non-Newtonian Fluid Mech.* 70 (1–2), 1–33.
- Bender, J.W., Wagner, N.J., 1995. Optical measurement of the contributions of colloidal forces to the rheology of concentrated suspensions. *J. Colloid Interface Sci.* 172 (1), 171–184.
- Bhagath Singh, G.V., Subramaniam, K.V.L., 2017. Evaluation of sodium content and sodium hydroxide molarity on compressive strength of alkali activated low-calcium fly ash. *Cement Concr. Compos.* 81, 122–132.
- Bhagath Singh, G.V., Subramaniam, K.V.L., 2019. Influence of processing temperature on the reaction product and strength gain in alkali-activated fly ash. *Cement Concr. Compos.* 95, 10–18.
- Bhagath Singh, G.V., Subrahmanyam, C., Subramaniam, K.V.L., 2018. Dissolution of the glassy phase in low-calcium fly ash during alkaline activation. *Adv. Cem. Res.* 30 (7), 313–322.
- Burgos-Montes, O., Palacios, M., Rivilla, P., Puertas, F., 2012. Compatibility between superplasticizer admixtures and cements with mineral additions. *Constr. Build. Mater.* 31, 300–309.
- Chateau, X., Ovarlez, G., Trung, K.L., 2008. Homogenization approach to the behavior of suspensions of noncolloidal particles in yield stress fluids. *J. Rheol.* 52 (2), 489–506.
- Choi, M., Park, K., Oh, T., 2016. Viscoelastic properties of fresh cement paste to study the flow behavior. *International Journal of Concrete Structures and Materials* 10 (3), 65–74.
- Criado, M., Palomo, A., Fernández-Jiménez, A., Banfill, P.F.G., 2009. Alkali activated fly ash: effect of admixtures on paste rheology. *Rheol. Acta* 48 (4), 447–455.
- Dai, S.C., Bertevras, E., Qi, F., Tanner, R.I., 2013. Viscometric functions for noncolloidal sphere suspensions with Newtonian matrices. *J. Rheol.* 57 (2), 493–510.
- Deng, S.C., Zhang, X.B., Qin, Y.H., Luo, G.X., 2007. Rheological characteristic of cement clean paste and flowing behavior of fresh mixing concrete with pumping in pipeline. *J. Cent. South Univ. Technol.* 14 (1), 462.
- Duxson, P., Fernández-Jiménez, A., Provis, J.L., Lukey, G.C., Palomo, A., van Deventer, J.S., 2007. Geopolymer technology: the current state of the art. *J. Mater. Sci.* 42 (9), 2917–2933.
- Ferron, R.P.D., 2008. Formwork Pressure of Self-Consolidating Concrete: Influence of Flocculation Mechanisms, Structural Rebuilding, Thixotropy and Rheology. Doctoral dissertation. Northwestern University.
- Ferron, R.P., Gregori, A., Sun, Z., Shah, S.P., 2007. Rheological method to evaluate structural buildup in self-consolidating concrete cement pastes. *ACI Mater. J.* 104 (3), 242.
- Feys, D., Verhoeven, R., De Schutter, G., 2007. Evaluation of time independent rheological models applicable to fresh self-compacting concrete. *Appl. Rheol.* 17 (5), 56244–57190.
- Foss, D.R., Brady, J.F., 2000. Structure, diffusion and rheology of Brownian suspensions by Stokesian dynamics simulation. *J. Fluid Mech.* 407, 167–200.
- Frigaard, I.A., Paso, K.G., de Souza Mendes, P.R., 2017. Bingham's model in the oil and gas industry. *Rheol. Acta* 56 (3), 259–282.
- Joshi, A., Montes, C., Salehi, S., Allouche, E., Lvov, Y., 2015. Optimization of geopolymer properties by coating of fly-ash microparticles with nanoclays. *J. Inorg. Organomet. Polym. Mater.* 25 (2), 282–292.
- Kantro, D.L., 1980. Influence of water-reducing admixtures on properties of cement paste—a miniature slump test. *Cem. Concr. Aggregates* 2 (2), 95–102.
- Kim, J.H., Yim, H.J., Ferron, R.D., 2016. In situ measurement of the rheological properties and agglomeration on cementitious pastes. *J. Rheol.* 60 (4), 695–704.
- Kim, J.H., Kwon, S.H., Kawashima, S., Yim, H.J., 2017. Rheology of cement paste under high pressure. *Cement Concr. Compos.* 77, 60–67.
- Kong, X., Zhang, Y., Hou, S., 2013. Study on the rheological properties of Portland cement pastes with polycarboxylate superplasticizers. *Rheologica Acta* 52 (7), 707–718.
- Laskar, A.I., Bhattacharjee, R., 2011. Rheology of fly-ash-based geopolymer concrete. *ACI Mater. J.* 108 (5).
- Li, L., Usui, H., Suzuki, H., 2002. Study of pipeline transportation of dense fly ash-water slurry. *Coal Prep.* 22 (2), 65–80.
- Lin, Y., Phan-Thien, N., Khoo, B.C., 2015. Shear induced organization of particles in non-colloidal suspensions in steady shear flow. *J. Non-Newtonian Fluid Mech.* 223, 228–232.
- Lootens, D., Hébraud, P., Lécolier, E., Van Damme, H., 2004. Gelation, shear-thinning and shear-thickening in cement slurries. *Oil Gas Sci. Technol.* 59 (1), 31–40.
- Lowke, D., Gehlen, C., 2017. The zeta potential of cement and additions in cementitious suspensions with high solid fraction. *Cement Concr. Res.* 95, 195–204.
- Montes, C., Allouche, E., 2013. Rheological behavior of fly-ash-based geopolymers. In: *Geopolymer Binder Systems*. ASTM International.
- Montes, C., Zang, D., Allouche, E.N., 2012. Rheological behavior of fly ash-based geopolymers with the addition of superplasticizers. *Journal of Sustainable Cement-Based Materials* 1 (4), 179–185.
- Mucsi, G., Szczeni, Á., Nagy, S., 2018. Fiber reinforced geopolymer from synergetic utilization of fly ash and waste tire. *J. Clean. Prod.* 178, 429–440.
- Nair, S.D., Ferron, R.D., 2016. Real time control of fresh cement paste stiffening:

- smart cement-based materials via a magnetorheological approach. *Rheol. Acta* 55 (7), 571–579.
- Olivas, A., Helsen, M.A., Martys, N.S., Ferraris, C.F., George, W.L., Ferron, R., 2016. Rheological Measurement of Suspensions without Slippage: Experiment and Model.
- Palacios, M., Houst, Y.F., Bowen, P., Puertas, F., 2009. Adsorption of superplasticizer admixtures on alkali-activated slag pastes. *Cement Concr. Res.* 39 (8), 670–677.
- Palomo, A., Krivenkob, P., Garcia-Lodeiro, I., Kavalerovab, E., Maltsevaa, O., Fernández-Jiménez, A., 2014. A review on alkaline activation: new analytical perspectives. *Mater. Construcción* 64 (315), 1–24. <https://doi.org/10.3989/mc.2014.00314>.
- Perrot, A., Mélinge, Y., Rangeard, D., Micaelli, F., Estellé, P., Lanos, C., 2012. Use of ram extruder as a combined rheo-tribometer to study the behavior of high yield stress fluids at low strain rate. *Rheol. Acta* 51 (8), 743–754.
- Pierre, A., Lanos, C., Estellé, P., 2013. Extension of spread-slump formulae for yield stress evaluation. *Appl. Rheol.* 23 (6), 63849.
- Provis, J., van Deventer, J.S.J., 2009. In: Provis, J., van Deventer, J.S.J. (Eds.), *Geopolymers, Structure, Processing, Properties and Industrial Applications*. Woodhead Publishing Limited, ISBN 978-1-84569-449-4.
- Ray, S., Dash, J., Devi, N., Sasmal, S., Pesala, B., 2015. March). Hydration kinetics of cement composites with varying water-cement ratio using terahertz spectroscopy. In: Terahertz, R.F., Millimeter (Eds.), *Submillimeter-Wave Technology and Applications VIII*, vol. 9362. International Society for Optics and Photonics, p. 936211.
- Roussel, N., Coussot, P., 2005. “Fifty-cent rheometer” for yield stress measurements: from slump to spreading flow. *J. Rheol.* 49 (3), 705–718.
- Roussel, N., Ovarlez, G., Garrault, S., Brumaud, C., 2012. The origins of thixotropy of fresh cement pastes. *Cement Concr. Res.* 42 (1), 148–157.
- Saak, A.W., Jennings, H.M., Shah, S.P., 2001. The influence of wall slip on yield stress and viscoelastic measurements of cement paste. *Cement Concr. Res.* 31 (2), 205–212.
- Saak, A.W., Jennings, H.M., Shah, S.P., 2004. A generalized approach for the determination of yield stress by slump and slump flow. *Cement Concr. Res.* 34 (3), 363–371.
- Singh, A., Nott, P.R., 2003. Experimental measurements of the normal stresses in sheared Stokesian suspensions. *J. Fluid Mech.* 490, 293–320.
- Subramaniam, K.V., Wang, X., 2010. An investigation of microstructure evolution in cement paste through setting using ultrasonic and rheological measurements. *Cement Concr. Res.* 40 (1), 33–44.
- Tan, Z., Bernal, S.A., Provis, J.L., 2017. Reproducible mini-slump test procedure for measuring the yield stress of cementitious pastes. *Mater. Struct.* 50 (6), 235.
- Tattersall, G.H., Banfill, P.F., 1983. *The Rheology of Fresh Concrete* (No. Monograph).
- Termkhajornkit, P., Nawa, T., 2004. The fluidity of fly ash–cement paste containing naphthalene sulfonate superplasticizer. *Cement Concr. Res.* 34 (6), 1017–1024.
- Van Zijl, G.P., Paul, S.C., Tan, M.J., 2016. Properties of 3d Printable Concrete.
- Vance, K., Dakhane, A., Sant, G., Neithalath, N., 2014. Observations on the rheological response of alkali activated fly ash suspensions: the role of activator type and concentration. *Rheol. Acta* 53 (10–11), 843–855.
- Vázquez-Quesada, A., Tanner, R.I., Ellero, M., 2016. Shear thinning of noncolloidal suspensions. *Phys. Rev. Lett.* 117 (10), 108001.
- Wallevik, J.E., 2005. Thixotropic investigation on cement paste: experimental and numerical approach. *J. Non-Newtonian Fluid Mech.* 132 (1–3), 86–99.
- Wang, X., Subramaniam, K.V., 2011. Ultrasonic monitoring of capillary porosity and elastic properties in hydrating cement paste. *Cement Concr. Compos.* 33 (3), 389–401.
- Yang, X., Zhu, W., Yang, Q., 2008. The viscosity properties of sodium silicate solutions. *J. Solut. Chem.* 37 (1), 73–83.
- Yotsumoto, H., Yoon, R.H., 1993. Application of extended DLVO theory: II. Stability of silica suspensions. *J. Colloid Interface Sci.* 157 (2), 434–441.
- Yuan, Q., Zhou, D., Khayat, K.H., Feys, D., Shi, C., 2017. On the measurement of evolution of structural build-up of cement paste with time by static yield stress test vs. small amplitude oscillatory shear test. *Cement Concr. Res.* 99, 183–189.
- Zarraga, I.E., Hill, D.A., Leighton Jr., D.T., 2000. Erratum: “The characterization of the total stress of concentrated suspensions of noncolloidal spheres in Newtonian fluids” (*J. Rheol.* 44, 185–220 (2000)). *J. Rheol.* 44 (3), 671–671.
- Zhuang, X.Y., Chen, L., Komarneni, S., Zhou, C.H., Tong, D.S., Yang, H.M., et al., 2016. Fly ash-based geopolymer: clean production, properties and applications. *J. Clean. Prod.* 125, 253–267.